Low-temperature *in situ* cleaning of silicon (100) surface by electron cyclotron resonance hydrogen plasma

Heung-Sik Tae,[a] Sang-June Park,[b] Seok-Hee Hwang,[a] Ki-Hyun Hwang,[b] Euijoon Yoon,[b] and Ki-Woong Whang[a]
Inter-university Semiconductor Research Center (ISRC), Seoul National University, Seoul 151-742, Korea

Se Ahn Song
Samsung Advanced Institute of Technology, Suwon 440-600, Korea

(Received 1 August 1994; accepted 30 March 1995)

Low-temperature, defect-free, *in situ* cleaning of silicon prior to homoepitaxy is successfully developed by an electron cyclotron resonance hydrogen plasma treatment in an ultrahigh vacuum chamber. The plasma potential distribution was measured by a Langmuir probe method to understand the effect of the substrate dc bias during hydrogen plasma cleaning. It changes from downhill to uphill distribution as the dc bias changes from a negative to a positive value, which leads to a decrease in the ion number density arriving at the substrate and results in the complete suppression of the defect formation in the Si substrate. *In situ* hydrogen plasma cleaned Si wafer always resulted in higher quality epilayers than ones cleaned only by so-called hydrogen passivation after the HF dip. We found that there is a critical dose of the hydrogen ions during *in situ* plasma cleaning beyond which crystalline defects are observed in the Si substrate, subsequently leading to the poor crystallinity of the epilayers. The dose of the hydrogen ions during plasma cleaning can be effectively controlled by the substrate dc bias, the microwave power, the magnet current, and the cleaning time. © *1995 American Vacuum Society.*

I. INTRODUCTION

Low-temperature Si and SiGe epitaxy for high-speed heterojunction bipolar transistors (HBTs) and for very large scale integration (VLSI) requires a complete removal of native oxide and hydrocarbon contaminants on the Si surface prior to epitaxy at low temperatures without damaging the surface. Conventional thermal cleaning in high-temperature epitaxy is not adequate in these applications and the effective low-temperature cleaning techniques have been sought ever since. A low-temperature cleaning by hydrogen passivation after HF dip has been used for the fabrication of the SiGe HBT.[1] However, when the hydrogen passivation is not perfect, there is an appreciable concentration of adsorbed impurities on the Si surface and they lead to defective epitaxial layers,[2] and it is hard to get reproducible results.

Plasma cleaning is known to be an effective way of removing surface contaminants at low temperatures (<600 °C).[3,4] Conventional plasma cleaning utilizes the physical sputtering by Ar ions, and the ion-induced damage must be annealed dynamically at considerably high temperatures (~800 °C) to ensure defect-free epitaxy.[5] Hydrogen plasma cleaning, on the other hand, is known as a *chemical* etching[6] by lighter hydrogen atoms and ions, and it has been used as a substitute for Ar plasma cleaning.[6,7] However, the defect formation in Si wafer is reported when the wafer is exposed to hydrogen-containing plasmas at low temperatures in a non-UHV system.[8,9] A remote hydrogen plasma cleaning is devised to remove the native oxide without plasma damage, but even in remote plasma configuration defect formation was reported at some conditions, possibly by ion impingement.[7]

We previously reported that a 2 min electron cyclotron resonance (ECR) hydrogen plasma cleaning at 560 °C is severe enough to generate crystalline defects in Si substrates, and it was possible to suppress the defect formation by applying +10 V to the substrate during *in situ* cleaning.[10] We further explore the effects of other process parameters during *in situ* hydrogen plasma cleaning such as the microwave power, the distance between the ECR layer and the substrate, etc. We found that there is a critical dose of hydrogen ions during *in situ* plasma cleaning before crystalline defects are observed in Si substrates. The role of hydrogen ions in defect formation is discussed, and experimental results are given to support the idea.

II. EXPERIMENT

The experimental apparatus (Fig. 1) used in this experiment is basically the same as that previously described.[10] Briefly, its base pressure is 1×10^{-9} Torr and it is possible to produce a high-density plasma at a low pressure of 10^{-4} Torr with the electron cyclotron resonance plasma. A TE_{113} mode ECR cavity and the magnets are designed to make ECR layer (875 G line) as parallel as possible to the substrates. High-purity (99.9999%) hydrogen is introduced to the ECR cavity and the reactant gases are introduced through a gas dispersal ring. Energy and flux of the incident ions can be controlled in this system by changing the input microwave power, the position of the ECR layer from the substrate, the operating pressure, and the substrate dc bias.

[a]Also with the Department of Electrical Engineering.
[b]Also with the Department of Inorganic Materials Engineering.

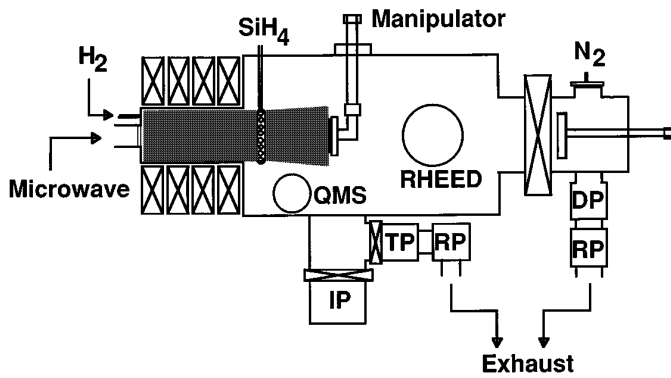

FIG. 1. The schematic diagram of the UHV–ECRCVD system.

A. Effect of process parameters on the energy and flux of the incident ion

Figure 2 shows the changes in the plasma density and the temperatures of the electrons and ions in the plasma with input microwave power, as measured by a Langmuir probe and an ion energy analyzer positioned approximately 2 cm from the substrate. As the microwave power increases, the plasma density increases linearly, but temperatures of the ions and electrons do not change substantially. Figure 3 shows the changes in B-field magnitude with the distance from the ECR cavity at different magnet currents. The ECR layers at 875 G are marked by arrows and they move away from the substrate as the magnet current decreases. The microwave propagation direction and B-field lines are parallel in this magnet-cavity configuration, and the maximum plasma density occurs at the ECR layer. The B-field intensity decreases towards the substrate, and the guiding center of electrons drift along the B-field line due to $-\mu\nabla B$ force, where μ is the magnetic moment of the gyrating particles. An ambipolar space-charge potential develops as a result of the different drift velocity of ion and electron, and ions are driven downstream towards the substrate by the electric field. As the ions travel along the B-field line, the potential energy is converted to the kinetic energy. But, as shown in Fig. 3, the gradient of magnetic field in our system is moderate and consequently, it is believed that the converted kinetic energy of ions is in the order of plasma potential energy when they arrive at the substrate. On the other hand, the average ion energy decreases due to charge exchange and elastic collisions with neutrals[11,12] as ions travel down. As a result, the energy and the flux of the hydrogen ions decrease as the ECR layer moves away from the substrate.

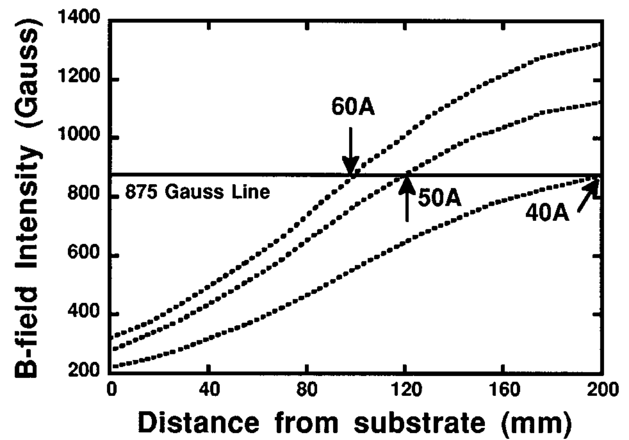

FIG. 3. The changes in B-field intensity with distance from the substrate at various magnet currents. The positions of the ECR layers (875 G) at different magnet current conditions are indicated with arrows.

We measured the plasma potential distribution near the sheath boundary by a Langmuir probe. Sheath potential is kept relatively unchanged with the substrate dc bias as shown in Fig. 4. The plasma potential near the sheath boundary increases with the application of a positive dc bias, contrary to the expectation that the sheath potential will decrease with a positive dc bias, while the plasma potential near the sheath boundary is kept unchanged. The reason for this is that the area of the substrate is large enough to affect the bulk plasma, since it draws significant amount of electrons from the plasma. The sheath potential should be kept constant to keep the quasineutrality of the plasma. The detailed mechanism of the energy conversion of the incident ions

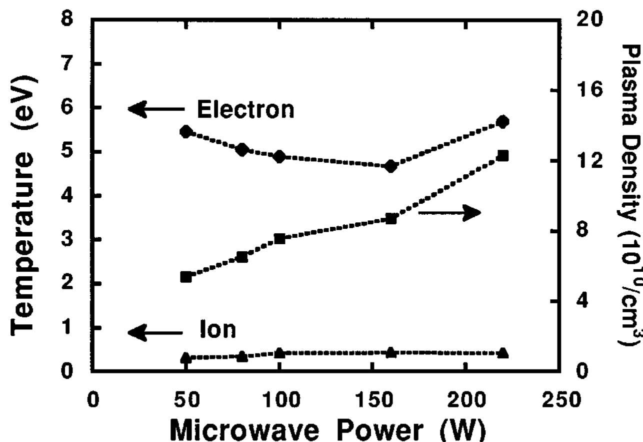

FIG. 2. The changes in plasma density, ion temperature, and electron temperature with microwave power. The probe is positioned at the center and at 2 cm from the substrate.

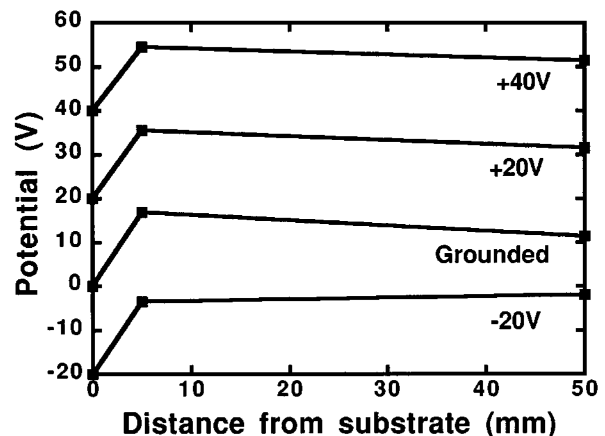

FIG. 4. Plasma potential distribution at various substrate dc biases. Note the slope changes from downhill at -20 V to uphill at grounded and positive biases.

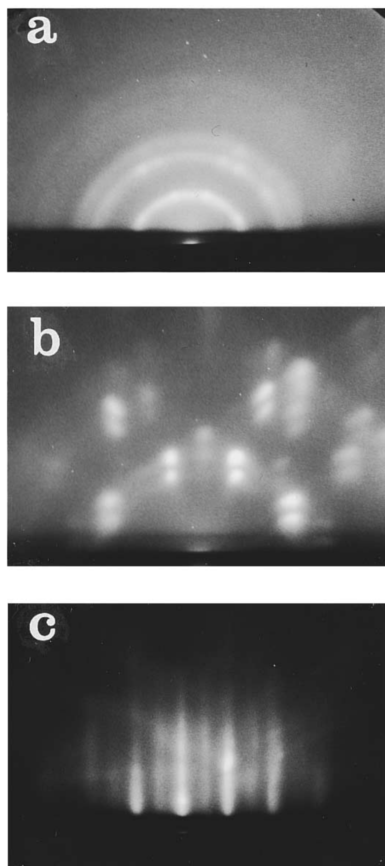

FIG. 5. RHEED patterns of the Si epilayers grown at the same conditions after three different pregrowth treatments, demonstrating the effect of the *in situ* hydrogen plasma cleaning. Deposition temperature 560 °C, microwave power 50 W, magnet current 40 A, growth pressure 1.5×10^{-3} Torr, deposition time 285 min. (a) 30 min air exposure after HF dip, and no hydrogen plasma cleaning, (b) immediate loading after HF dip, and no hydrogen plasma cleaning, (c) immediate loading after HF dip, and *in situ* hydrogen plasma cleaning.

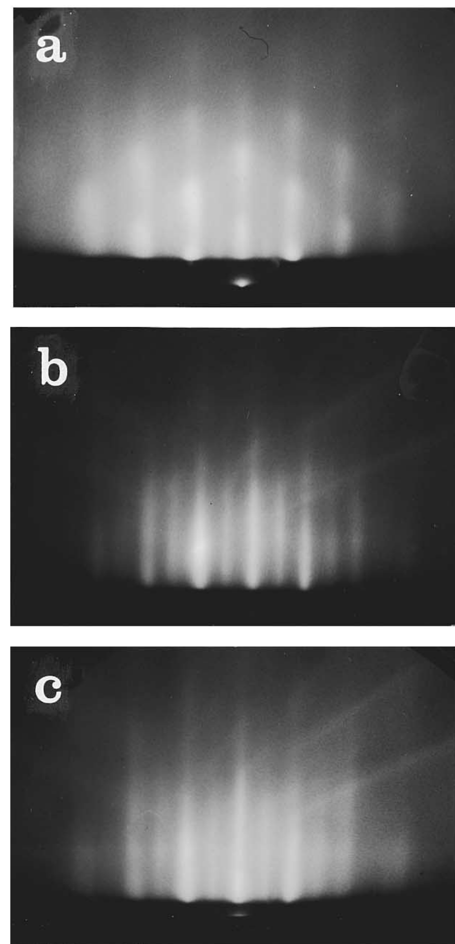

FIG. 6. RHEED patterns of the *in situ* hydrogen plasma cleaned Si substrates at various substrate dc bias conditions. (a) −50 V, (b) floating, and (c) +10 V. Other cleaning conditions such as the substrate temperature, the microwave power, the magnet current, the hydrogen flow rate, the total pressure, the cleaning time are kept the same at 560 °C, 100 W, 50 A, 74 sccm, 8×10^{-4} Torr, and 2 min, respectively.

with dc bias in our ECR system will be reported elsewhere.[13] The changes in incident ion energy flux are not due to the decrease in sheath potential, but they are caused by the plasma potential distribution change from downhill to uphill distribution as the dc bias changes from a negative to a positive value, and the decrease in the ion number density arriving at the substrate.

B. Need for *in situ* hydrogen plasma cleaning of Si(100) wafers

The samples used in this experiment are 4-in-diam, n-type (100) Si wafer (resistivity, 10–20 Ω cm). These wafers are *ex situ* cleaned at 120 °C with a 4:1 H_2SO_4:H_2O_2 solution for 10 min and rinsed with de-ionized water for 6 min, and subsequently dipped into a 10:1 HF solution for 30 s for the complete removal of the surface oxide. The wafers are transferred immediately to the growth chamber through a nitrogen-purged load-lock.

Figure 5 shows reflection high-energy electron diffraction (RHEED) patterns for the epitaxial layers grown at the same condition except the *in situ* cleaning step. Sample (a) is cleaned by HF dip and no DI water rinse, and subsequently exposed to air for 30 min, then loaded into the growth chamber. Sample (b) is cleaned by HF dip and no DI water rinse, and immediately loaded into the growth chamber. Sample (c) is cleaned by HF dip and *in situ* cleaned by hydrogen plasma for 2 min. The epilayer grown after 30 min air exposure is polycrystalline, and the fast-loaded sample after HF dip is a single crystal with a high density of defects. The reason for the poor crystallinity of (a) and (b) comes from the incomplete hydrogen passivation and contaminants adsorbed on the cleaned Si surface. On the other hand, the epilayer grown after *in situ* hydrogen plasma cleaning is always a single crystal with a well-defined 2×1 RHEED surface reconstruction pattern, clearly demonstrating the effectiveness of *in situ* hydrogen plasma cleaning.

III. RESULTS AND DISCUSSION

A. Effect of the substrate dc bias

Plasma cleaning is studied at a substrate temperature of 560 °C, microwave power of 100 W, magnet current of 50 A, hydrogen flow rate of 74 sccm, and pressure of 8×10^{-4} Torr. Figure 6 shows the changes in RHEED pattern with the sub-

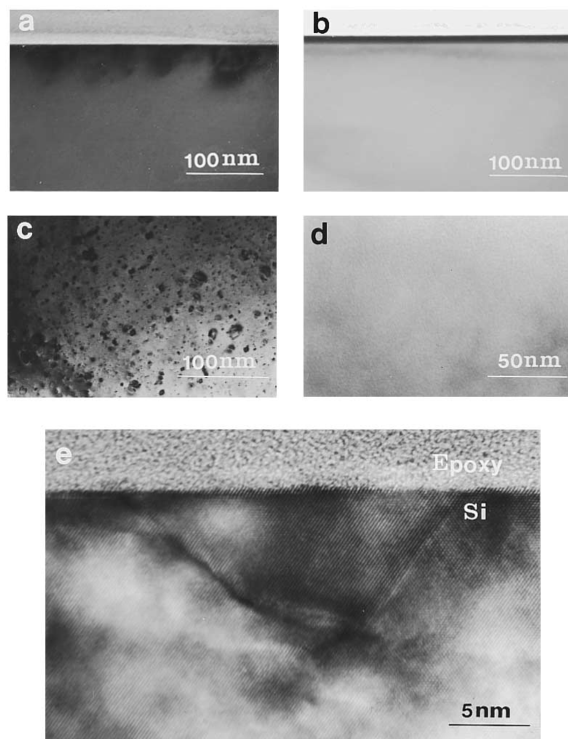

FIG. 7. TEM micrographs for the Si surfaces after 2 min *in situ* hydrogen plasma cleaning at floating potential and at +10 V substrate dc bias. (a) Bright-field (BF) XTEM at floating potential, (b) BF XTEM at +10 V, (c) BF plan-view TEM at floating, (d) BF plan-view TEM at +10 V, (e) HR-TEM of the defects shown in (a).

strate dc bias after 2 min hydrogen plasma cleaning. At −50 V, faint half-order streaks are seen as in Fig. 6(a), but integral order streaks are spotty and discrete, implying that the Si surface becomes rough after energetic hydrogen-ion bombardment. Figures 6(b) and 6(c) show the 2×1 surface reconstruction after 2 min hydrogen plasma exposure. Both streaky RHEED patterns with 2×1 surface reconstruction imply that the surfaces are smooth and free of native oxide at floating and +10 V biased conditions, respectively. But the RHEED is insensitive to the presence of crystal defects in the bulk. Figures 7(a) and 7(b) are cross-section transmission electron microscopy (XTEM) photographs of Si substrate cleaned at floating and +10 V biased conditions, respectively. Figures 7(c) and 7(d) are the corresponding plan-view TEM photographs. At floating condition, the substrate is full of defects ($\sim 10^{10}/cm^3$) which are believed to be dislocation loops, defect clusters of varying sizes. The high-resolution TEM (HRTEM) photograph of the defects, however, is rather complex. {111}-type planar defects are clearly seen, and it was proposed that they are originated from the condensation of excess hydrogen in Si along {111} planes.[8,9]

Crystalline defect formation in Si substrates during hydrogen plasma cleaning is presumed to be caused by hydrogen penetration into Si. The possible defect generators are hydrogen atoms, or ions, or both. Jeng *et al.* measured the hydrogen concentration in Si as high as $10^{20}/cm^3$ by secondary-ion mass spectrometry (SIMS) after hydrogen-containing plasma exposure, and reported the similar planar defects.[9] If the penetration of hydrogen is purely by thermal diffusion of hydrogen atoms from the gas to the Si, the hydrogen concentration profile and the defect formation will remain unaffected by the substrate dc bias. The fact that the substrate dc bias influences the defect formation strongly supports the idea that the defect formation during hydrogen plasma cleaning is mainly caused by hydrogen ions. Recent results from Zhou *et al.*[14] and Nakashima *et al.*[15] clearly show the essential role of hydrogen ions in oxide removal, hydrogen penetration, and formation of defects in Si. They both found that the hydrogen ion must be present to remove the native oxide on Si at low temperatures, and to get noticeable hydrogen penetration into Si. Our result of complete oxide removal and even defect formation after only 2 min exposure at 560 °C and at floating potential demonstrates clearly that there are numerous hydrogen ions impinging on the Si surface in our ECR system. Ion current density measurement in similarly configured ECR systems show that there are considerable ion fluxes to the substrate.[16,17]

In a similar *in situ* cleaning by remote radio-frequency hydrogen plasma, it is reported that it takes much longer time of 30–60 min to remove the native oxide.[2] This comparatively slow etch rate of the native oxide results from the lower density of hydrogen ions at higher pressure than that of ECR plasma, and also from the remoteness of the plasma source, though it is claimed that the cleaning is made by hydrogen atoms. Once the damaging species are identified, it is possible to suppress the ion damages by applying positive bias to the substrate. As shown in Figs. 7(b) and 7(d), the application of +10 V dc bias to the substrate during hydrogen plasma cleaning eliminates the defect formation completely.

When +10 V is applied to the substrate, the plasma density of the bulk plasma does not change since the microwave plasma power and the operating pressure are unchanged. But the plasma potential near the sheath boundary changes from downhill distribution at floating condition to uphill distribution at positively biased condition as shown in Fig. 4, thus the energy and the flux of the ions decreases with dc bias, resulting in the suppression of the defect formation.

B. Effects of other process parameters

The effects of other process parameters such as microwave power, the position of the ECR layer, cleaning time, etc., on defect formation is studied. We already know that defects are observed in Si after the plasma cleaning for 2 min at floating condition (substrate temperature 560 °C, microwave power 100 W, magnet current 50 A). Plasma cleaning for 2 min at floating condition at a reduced microwave power (50 W) or at a remoter ECR layer position (magnet current, 40 A), however, do not produce crystalline defects in Si as observed by plan-view TEM [Figs. 8(a) and 8(c), respectively]. When the microwave power is reduced from 100 to 50 W, the bulk plasma density is reduced from 8×10^{10} to $5\times10^{10}/cm^3$, consequently flux of the hydrogen ion is reduced. When the magnet current decreases from 50 to 40 A, the distance from the substrate to the ECR layer increases from 12 to 20 cm, resulting in the decrease of ion energy as ions travel further downstream.

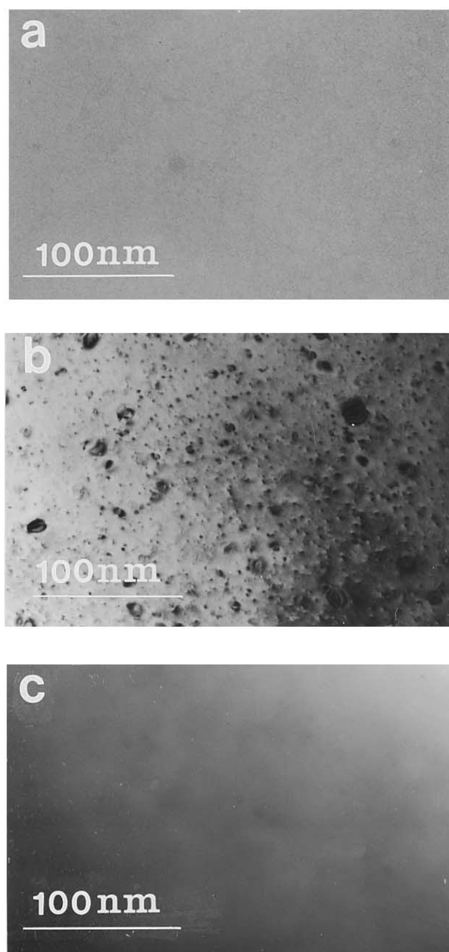

FIG. 8. BF TEM micrographs showing the effect of the process parameters on the defect formation in the Si substrate after 2 min *in situ* hydrogen plasma cleaning at floating potential, substrate temperature of 560 °C. (a) Microwave power 50 W, magnet current 50 A; (b) microwave power 100 W, magnet current 50 A; (c) microwave power 100 W, magnet current 40 A.

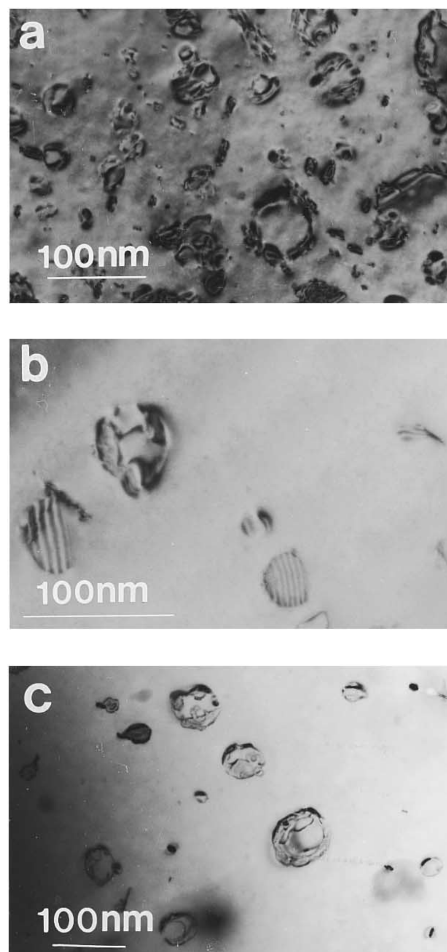

FIG. 9. BF TEM micrographs showing the effect of the process parameters on the defect formation in the Si substrate after 20 min *in situ* hydrogen plasma cleaning at +10 V substrate dc bias, substrate temperature of 560 °C. (a) Microwave power 150 W, magnet current 50 A; (b) microwave power 100 W, magnet current 50 A; (c) microwave power 100 W, magnet current 60 A.

When the Si substrates are exposed longer (20 min), though at no-defect condition at 2 min (plasma power 100 W, magnet current 50 A, substrate dc bias +10 V), we begin to observe similar defects by plan-view TEM as shown in Fig. 9(b). The hydrogen ion flux towards the Si substrate during cleaning is the same in both cases, since the *in situ* hydrogen plasma cleaning condition is the same. However, the total doses, i.e., flux times cleaning time, of the hydrogen ions are ten times different. It is now estimated that there is a critical dose[18] of hydrogen ions between two exposures (2 min exposure and 20 min exposure) where the crystalline defects accumulate, coalesce and begin to appear as platelets, dislocation loops, and defect clusters in TEM observation. Defect density ($\sim 10^8/\mathrm{cm}^2$) of the 20 min cleaned sample is two orders of magnitude lower than that of the sample cleaned for 2 min at floating condition ($\sim 10^{10}/\mathrm{cm}^2$) of Fig. 7(c), but is still detrimental. When the microwave power increases to 150 W, the defect density increases to $10^9/\mathrm{cm}^2$ as in Fig. 9(a). On the other hand, when the magnet current increases from 50 to 60 A, the ECR layer shifts only 2 cm towards the substrate and the defect density barely changes.

The judgment of the extent of *in situ* hydrogen plasma cleaning is often done by RHEED only, but it is hard to quantify the completeness of the cleaning. The plasma-cleaned surface for the successful epitaxy should be free not only from ion damage but also from surface contamination. In the previous discussion it is found that the RHEED alone cannot tell the presence of ion damage. Likewise, the RHEED alone cannot judge the surface cleanliness. Any *in situ* surface analytical tools may help in the judgment, but often their resolution is not satisfactory. One of the most sensitive ways to judge the surface cleanliness is to grow epitaxial layers on the cleaned surface. Epitaxial growth itself after various *in situ* cleaning steps reveals every minute details of the surface contamination and imperfection. Thus, we deposited 300-Å-thick Si epitaxial layers for 90 min at the same growth conditions, after hydrogen *in situ* plasma cleaning at various conditions. We know that this growth condition does not produce any defects in Si epilayers even after 285 min growth.[10] When the substrate is biased at −50 V during 2 min plasma cleaning, the RHEED pattern is spotty as shown in Fig. 6(a). The epilayer on this surface is a single crystal with a high density of microtwins, as shown in

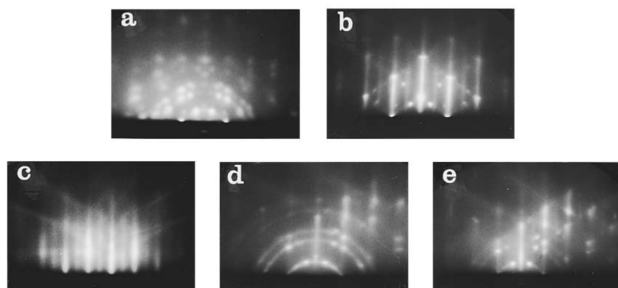

FIG. 10. RHEED patterns for the Si epilayers at the same growth condition after the *in situ* hydrogen plasma cleanings at various substrate dc biases. The epitaxial growth conditions are kept the same at 560 °C, 100 W, 50 A, +50 V dc bias and the total pressure of 1.5×10^{-3} Torr. Substrate dc bias conditions during *in situ* cleaning are (a) −50 V, (b) floating, (c) +10 V, (d) +50 V, (e) +100 V.

Fig. 10(a), presumably caused by defects in the substrate which is already heavily damaged during cleaning. At floating condition, the result is similar, and we begin to see half-order streaks with spotty integral order streaks [Fig. 10(b)]. Figures 10(c), 10(d), and 10(e) show RHEED patterns of the epilayers grown after 2 min *in situ* cleaning at +10, +50, +100 V dc biases, respectively. When the substrate is excessively biased (+50, +100 V), the RHEED patterns are a mixture of streaks and rings. Polycrystallinity in this case is not due to ion damage, but the excessive bias during cleaning does not provide the sufficient hydrogen ion dose for complete removal of native oxide, which is the necessary condition for defect-free epitaxy. Extended cleaning at these conditions will complete the native oxide removal, and result in similar RHEED pattern for the epilayer grown after plasma cleaning for 2 min at the +10 V dc bias condition.

IV. CONCLUSION

In situ hydrogen plasma cleaning process at 560 °C is successfully developed in a UHV–ECR CVD. The subtleties of the hydrogen plasma cleaning is investigated by RHEED, TEM of the cleaned substrate itself, and crucially of the epilayers grown after various cleaning steps. ECR hydrogen plasma produces a high density of hydrogen ions, and effectively removes the native oxide in a relatively short time. Exposure of Si substrate beyond a critical dose makes crystalline defects to accumulate to an observable level, and it leads to a defective epilayer. Appearance of defects in the substrate after *in situ* cleaning is determined by the flux of the hydrogen ions and the cleaning time. Defect-free *in situ* hydrogen plasma cleaning is obtained by the proper control of the process parameters such as the microwave power, the substrate dc bias, the distance between the substrate and the ECR layer.

ACKNOWLEDGMENT

The authors would like to thank Korea Telecom Research Laboratories for their support for this work.

[1]E. F. Crabbe, J. H. Comfort, W. Lee, J. D. Cressler, B. S. Meyerson, A. C. Megdanis, J. Y.-C. Sun, and J. M. C. Stork, IEEE Electron Device Lett. **13**, 259 (1992).

[2]B. Anthony. L. Breaux, T. Hsu, S. Banerjee, and A. Tasch, J. Vac. Sci. Technol. B **7**, 621 (1989).

[3]M. Delfino, S. Salimian, D. Hodul, A. Ellingboe, and W. Tsai, J. Appl. Phys. **71**, 1001 (1992).

[4]M. Ishii, K. Nakashima, I. Tajima, and M. Yamamoto, Appl. Phys. Lett. **58**, 1378 (1991).

[5]J. H. Comfort, L. M. Gaverick, and R. Reif, J. Appl. Phys. **62**, 3388 (1987); L. M. Gaverick, J. H. Comfort, T. R. Yew, R. Reif, F. A. Baiocchi, and H. S. Luftman, *ibid.* **62**, 3398 (1987).

[6]H. Yamada, J. Appl. Phys. **65**, 775 (1989).

[7]T. Hsu, B. Anthony, R. Qian, J. Irby, S. Banerjee, A. Tasch, S. Lin, H. Marcus, and C. Magee, J. Electron. Mater. **20**, 279 (1991).

[8]N. M. Johnson, F. A. Ponce, R. A. Street, and R. J. Nemanich, Phys. Rev. B **35**, 4166 (1987).

[9]S. J. Jeng, G. S. Oehrlein, and G. J. Scilla, Appl. Phys. Lett. **53**, 31 (1988).

[10]H.-S. Tae, S.-H. Hwang, S.-J. Park, E. Yoon, and K.-W. Whang, Appl. Phys. Lett. **64**, 1021 (1994).

[11]Y. P. Raizer, *Gas Discharge Physics* (Springer, New York, 1987).

[12]J. H. Simons, G. M. Fontana, H. T. Francis, and L. G. Unger, J. Chem. Phys. **11**, 312 (1943).

[13]H.-S. Tae, S.-J. Park, S.-H. Hwang, E. Yoon, and K.-W. Whang (unpublished).

[14]Z.-H. Zhou, E. S. Aydil, R. A. Gottscho, Y. J. Chabal, and R. Reif, J. Electrochem. Soc. **140**, 3316 (1993).

[15]K. Nakashima, M. Ishii, T. Hayakawa, I. Tajima, and M. Yamamoto, J. Appl. Phys. **74**, 6936 (1993).

[16]S. M. Rossnagel, K. Schatz, S. J. Whitehair, R. C. Guarnieri, D. N. Ruzic, and J. J. Cuomo, J. Vac. Sci. Technol. A **9**, 702 (1991).

[17]K.-W. Whang, S.-H. Lee, and H.-J. Lee, J. Vac. Sci. Technol. A **10**, 1307 (1992).

[18]J. F. Gibbons, Proc. IEEE **60**, 1062 (1972).